SIAM J. SCI. COMPUT.
Vol. 26, No. 6, pp. 2010–2028

A FOURTH-ORDER TIME-SPLITTING LAGUERRE–HERMITE PSEUDOSPECTRAL METHOD FOR BOSE–EINSTEIN CONDENSATES*

WEIZHU BAO† AND JIE SHEN‡

Abstract. A fourth-order time-splitting Laguerre–Hermite pseudospectral method is introduced for Bose–Einstein condensates (BECs) in three dimensions with cylindrical symmetry. The method is explicit, time reversible, and time transverse invariant. It conserves the position density and is spectral accurate in space and fourth-order accurate in time. Moreover, the new method has two other important advantages: (i) it reduces a three-dimensional (3-D) problem with cylindrical symmetry to an effective two-dimensional (2-D) problem; (ii) it solves the problem in the whole space instead of in a truncated artificial computational domain. The method is applied to vector Gross–Pitaevskii equations (VGPEs) for multicomponent BECs. Extensive numerical tests are presented for the one-dimensional (1-D) GPE, the 2-D GPE with radial symmetry, the 3-D GPE with cylindrical symmetry, as well as 3-D VGPEs for two-component BECs, to show the efficiency and accuracy of the new numerical method.

Key words. Gross–Pitaevskii equation, Bose–Einstein condensate, time-splitting, Laguerre–Hermite pseudospectral method, vector Gross–Pitaevskii equations

AMS subject classifications. 35Q55, 65T99, 65Z05, 65N12, 65N35, 81-08

DOI. 10.1137/030601211

1. Introduction.

Since its realization in dilute bosonic atomic gases [2, 12], Bose–Einstein condensation of alkali atoms and hydrogen has been produced and studied extensively in the laboratory [26], and it has spurred great excitement in the atomic physics community and renewed the interest in studying the collective dynamics of macroscopic ensembles of atoms occupying the same one-particle quantum state [17, 23]. Theoretical predictions of the properties of a Bose–Einstein condensate (BEC) such as the density profile [11], collective excitations [20], and the formation of vortices [33] can now be compared with experimental data [2]. Needless to say, this dramatic progress on the experimental front has stimulated a wave of activity on both the theoretical and the numerical front.

The properties of a BEC at temperatures T much smaller than the critical condensation temperature T_c [28] are usually well modeled by a nonlinear Schrödinger equation (NLSE), also called a Gross–Pitaevskii equation (GPE) [28, 32], for the macroscopic wave function which incorporates the trap potential as well as the interactions among the atoms. The effect of the interactions is described by a mean field which leads to a nonlinear term in the GPE. The cases of repulsive and attractive interactions—which can both be realized in the experiment—correspond to defocusing and focusing nonlinearities in the GPE, respectively. The results obtained by solving

*Received by the editors October 15, 2003; accepted for publication (in revised form) August 5, 2004; published electronically July 13, 2005.

http://www.siam.org/journals/sisc/26-6/60121.html

†Department of Computational Science, National University of Singapore, Singapore 117543 (bao@cz3.nus.edu.sg, http://www.cz3.nus.edu.sg/∼bao/). The research of this author was supported by National University of Singapore grant R-151-000-030-112.

‡Department of Mathematics, Purdue University, West Lafayette, IN 47907 (shen@math.purdue.edu). The research of this author was supported by NSF DMS-0311915 and the OAP (Fellow-Inbound) Programme supported by A*STAR and National University of Singapore.

the GPE showed excellent agreement with most of the experiments. (For a review see [3, 16].) In fact, up to now there have been very few experiments in ultracold dilute bosonic gases which could not be described properly by using theoretical methods based on the GPE [22, 27]. Thus developing efficient numerical methods for solving the GPE is very important in numerical simulation of BEC.

Recently, a series of numerical studies have been devoted to the numerical solution of the time-independent GPE for finding the ground states and of the time-dependent GPE for determining the dynamics of BECs. To compute ground states of BECs, Bao and Du [5] presented a continuous normalized gradient flow with diminishing energy and discretized it by a backward Euler finite difference method; Bao and Tang [8] proposed a method which can be used to compute the ground and excited states via directly minimizing the energy functional; Edwards and Burnett [19] introduced a Runge–Kutta-type method; other methods include an explicit imaginary-time algorithm in [1, 15], a direct inversion in the iterated subspace in [35], and a simple analytical-type method in [18]. To determine the dynamics of BECs, Bao, Jaksch, and Markowich [9], Bao [4], and Bao and Jaksch [10] presented a time-splitting spectral (TSSP) method, Ruprecht et al. [34] used the Crank–Nicolson finite difference (CNFD) method, and Cerimele et al. [13] and Cerimele, Pistella, and Succi [14] proposed a particle-inspired scheme.

In most experiments of BECs, the magnetic trap is with cylindrical symmetry. Thus, the three-dimensional (3-D) GPE in a Cartesian coordinate can be reduced to an effective two-dimensional (2-D) problem in a cylindrical coordinate. In this case, both the TSSP [9, 10, 4] and CNFD [34] methods have serious drawbacks: (i) One needs to replace the original whole space by a truncated computational domain with an artificial (usually homogeneous Dirichlet boundary conditions are used) boundary condition. How to choose an appropriate bounded computational domain is a difficult task in practice: if it is too large, the computational resource is wasted; if it is too small, the boundary effect will lead to wrong numerical solutions. (ii) The TSSP method is explicit and of spectral accuracy in space, but one needs to solve the original 3-D problem due to the periodic/homogeneous Dirichlet boundary conditions required by the Fourier/sine spectral method. Thus, the memory requirement is a big burden in this case. The CNFD method discretizes the 2-D effective problem directly, but it is implicit and only second-order accurate in space. The aim of this paper is to develop a numerical method which enjoys advantages of both the TSSP and the CNFD method. That is to say, the method is explicit and of spectral order accuracy in space, and it discretizes the effective 2-D problem directly. We shall present such an efficient and accurate numerical method for discretizing the 3-D GPE with cylindrical symmetry by applying a time-splitting technique and constructing appropriately scaled Laguerre–Hermite basis functions.

The paper is organized as follows. In section 2, we present the GPE and its dimension reduction. In section 3, we present time-splitting Hermite, Laguerre, and Laguerre–Hermite spectral methods for the one-dimensional (1-D) GPE, the 2-D GPE with radial symmetry, and the 3-D GPE with cylindrical symmetry, respectively. Extension of the time-splitting Laguerre–Hermite spectral method for vector Gross–Pitaevskii equations (VGPEs) for multicomponent BECs is presented in section 4. In section 5, numerical results for the 1-D GPE, the 2-D GPE with radial symmetry, the 3-D GPE with cylindrical symmetry, as well as 3-D VGPEs for multicomponent BECs, are reported to demonstrate the efficiency and accuracy of our new numerical methods. Some concluding remarks are given in section 6.

2. The GPE. At temperatures T much smaller than the critical temperature T_c [28], a BEC is well described by the macroscopic wave function $\psi = \psi(\mathbf{x}, t)$ whose evolution is governed by a self-consistent, mean field NLSE known as the GPE [24, 32]

$$i\hbar\frac{\partial\psi(\mathbf{x},t)}{\partial t} = -\frac{\hbar^2}{2m}\nabla^2\psi(\mathbf{x},t) + V(\mathbf{x})\psi(\mathbf{x},t) + NU_0|\psi(\mathbf{x},t)|^2\psi(\mathbf{x},t), \tag{2.1}$$

where m is the atomic mass, $\hbar$ is the Planck constant, N is the number of atoms in the condensate, and $V(\mathbf{x})$ is an external trapping potential. When a harmonic trap potential is considered, $V(\mathbf{x}) = \frac{m}{2}\left(\omega_x^2x^2 + \omega_y^2y^2 + \omega_z^2z^2\right)$, with ω_x, ω_y, and ω_z being the trap frequencies in the x-, y-, and z-directions, respectively. In most current BEC experiments, the traps are cylindrically symmetric, i.e., $\omega_x = \omega_y$. $U_0 = 4\pi\hbar^2a_s/m$ describes the interaction between atoms in the condensate with the s-wave scattering length a_s (positive for repulsive interaction and negative for attractive interaction). It is convenient to normalize the wave function by requiring

$$\int_{\mathbb{R}^3} |\psi(\mathbf{x},t)|^2\, d\mathbf{x} = 1. \tag{2.2}$$

In order to scale (2.1) under the normalization (2.2), we introduce

$$\tilde{t} = \omega_m t, \quad \tilde{\mathbf{x}} = \frac{\mathbf{x}}{a_0}, \quad \tilde{\psi}(\tilde{\mathbf{x}},\tilde{t}) = a_0^{3/2}\psi(\mathbf{x},t), \quad \text{with} \quad a_0 = \sqrt{\hbar/m\omega_m}, \tag{2.3}$$

where $\omega_m = \min\{\omega_x, \omega_y, \omega_z\}$, and a_0 is the length of the harmonic oscillator ground state. In fact, we choose $1/\omega_m$ and a_0 as the dimensionless time and length units, respectively. Plugging (2.3) into (2.1), multiplying by $1/m\omega_m^2a_0^{1/2}$, and then removing all $\tilde{}$, we get the following dimensionless GPE under the normalization (2.2) in three dimensions:

$$i\,\frac{\partial\psi(\mathbf{x},t)}{\partial t} = -\frac{1}{2}\nabla^2\psi(\mathbf{x},t) + V(\mathbf{x})\psi(\mathbf{x},t) + \beta\,|\psi(\mathbf{x},t)|^2\psi(\mathbf{x},t), \tag{2.4}$$

where $\beta = \frac{U_0N}{a_0^3\hbar\omega_m} = \frac{4\pi a_sN}{a_0}$ and

$$V(\mathbf{x}) = \frac{1}{2}\left(\gamma_x^2x^2 + \gamma_y^2y^2 + \gamma_z^2z^2\right), \text{ with } \gamma_\alpha = \frac{\omega_\alpha}{\omega_m}\ (\alpha = x, y, z).$$

There are two extreme regimes of the interaction parameter β: (1) $\beta = o(1)$, where (2.4) describes a weakly interacting condensation; (2) $\beta \gg 1$, where it corresponds to a strongly interacting condensation or to the semiclassical regime.

There are two typical extreme regimes between the trap frequencies: (1) $\gamma_x = 1$, $\gamma_y \approx 1$, and $\gamma_z \gg 1$, where it is a disk-shaped condensation; (2) $\gamma_x \gg 1$, $\gamma_y \gg 1$, and $\gamma_z = 1$, where it is a cigar-shaped condensation. In these two cases, the 3-D GPE (2.4) can be approximately reduced to a 2-D and 1-D equation, respectively [29, 9, 8], as explained below.

When $\omega_x \approx \omega_y$, $\omega_z \gg \omega_x$ ($\Longleftrightarrow \gamma_x = 1$, $\gamma_y \approx 1$, $\gamma_z \gg 1$), i.e., a disk-shaped condensation, following the procedure used in [8, 9, 29], the 3-D GPE can be reduced to a 2-D GPE [8, 9, 29]. Similarly, when $\omega_x \gg \omega_z$, $\omega_y \gg \omega_z$ ($\Longleftrightarrow \gamma_x \gg 1$, $\gamma_y \gg 1$, $\gamma_z = 1$), i.e., a cigar-shaped condensation, the 3-D GPE can be reduced to a 1-D GPE [8, 9, 29]. These suggest that we consider a GPE in d-dimension ($d = 1, 2, 3$):

$$\begin{aligned} &i\,\frac{\partial\psi(\mathbf{x},t)}{\partial t} = -\frac{1}{2}\nabla^2\psi + V_d(\mathbf{x})\psi + \beta_d\,|\psi|^2\psi, \quad \mathbf{x}\in\mathbb{R}^d,\\ &\psi(\mathbf{x},0) = \psi_0(\mathbf{x}), \qquad \mathbf{x}\in\mathbb{R}^d, \end{aligned} \tag{2.5}$$

with

$$\beta_d = \beta \begin{cases} \sqrt{\gamma_x\gamma_y}/2\pi, \\ \sqrt{\gamma_z/2\pi}, \\ 1, \end{cases} \qquad V_d(\mathbf{x}) = \begin{cases} \gamma_z^2 z^2/2, & d=1, \\ \left(\gamma_x^2 x^2 + \gamma_y^2 y^2\right)/2, & d=2, \\ \left(\gamma_x^2 x^2 + \gamma_y^2 y^2 + \gamma_z^2 z^2\right)/2, & d=3, \end{cases}$$

where $\gamma_x > 0$, $\gamma_y > 0$, and $\gamma_z > 0$ are constants. The normalization condition for (2.5) is

$$N(\psi) = \|\psi(\cdot,t)\|^2 = \int_{\mathbb{R}^d} |\psi(\mathbf{x},t)|^2 \, d\mathbf{x} \equiv \int_{\mathbb{R}^d} |\psi_0(\mathbf{x})|^2 \, d\mathbf{x} = 1. \tag{2.6}$$

3. Fourth-order time-splitting Laguerre–Hermite pseudospectral method. In this section we present a fourth-order time-splitting Laguerre–Hermite pseudospectral method for the problem (2.5) in three dimensions with cylindrical symmetry. As preparatory steps we begin by introducing the fourth-order time-splitting method and applying it with the Hermite pseudospectral method for the 1-D GPE and with the Laguerre pseudospectral method for the 2-D GPE with radial symmetry, respectively.

Consider a general evolution equation

$$iu_t = f(u) = Au + Bu, \tag{3.1}$$

where $f(u)$ is a nonlinear operator and the splitting $f(u) = Au + Bu$ can be quite arbitrary; in particular, A and B do not need to commute. For a given time step $\Delta t > 0$, let $t_n = n\ \Delta t$, $n = 0, 1, 2, \ldots$, and u^n be the approximation of $u(t_n)$. A fourth-order symplectic time integrator (cf. [41, 30]) for (3.1) is as follows:

$$\begin{aligned} &u^{(1)} = e^{-i2w_1 A\Delta t}\, u^n, \quad u^{(2)} = e^{-i2w_2 B\Delta t}\, u^{(1)}, \quad u^{(3)} = e^{-i2w_3 A\Delta t}\, u^{(2)}, \\ &u^{(4)} = e^{-i2w_4 B\Delta t}\, u^{(3)}, \quad u^{(5)} = e^{-i2w_3 A\Delta t}\, u^{(4)}, \quad u^{(6)} = e^{-i2w_2 B\Delta t}\, u^{(5)}, \\ &u^{n+1} = e^{-i2w_1 A\Delta t}\, u^{(6)}, \end{aligned} \tag{3.2}$$

where

$$\begin{aligned} &w_1 = 0.33780\ 17979\ 89914\ 40851,\ w_2 = 0.67560\ 35959\ 79828\ 81702, \\ &w_3 = -0.08780\ 17979\ 89914\ 40851,\ w_4 = -0.85120\ 71979\ 59657\ 63405. \end{aligned} \tag{3.3}$$

We now rewrite the GPE (2.5) in the form of (3.1) with

$$A\psi = \beta_d\, |\psi(\mathbf{x},t)|^2 \psi(\mathbf{x},t), \qquad B\psi = -\frac{1}{2}\nabla^2\psi(\mathbf{x},t) + V_d(\mathbf{x})\psi(\mathbf{x},t). \tag{3.4}$$

Thus, the key for an efficient implementation of (3.2) is to solve efficiently the following two subproblems:

$$i\,\frac{\partial\psi(\mathbf{x},t)}{\partial t} = A\psi(\mathbf{x},t) = \beta_d\, |\psi(\mathbf{x},t)|^2\psi(\mathbf{x},t), \qquad \mathbf{x}\in\mathbb{R}^d, \tag{3.5}$$

and

$$\begin{aligned} &i\,\frac{\partial\psi(\mathbf{x},t)}{\partial t} = B\psi(\mathbf{x},t) = -\frac{1}{2}\nabla^2\psi(\mathbf{x},t) + V_d(\mathbf{x})\psi(\mathbf{x}), \qquad \mathbf{x}\in\mathbb{R}^d, \\ &\lim_{|\mathbf{x}|\to+\infty} \psi(\mathbf{x},t) = 0. \end{aligned} \tag{3.6}$$

The decaying condition in (3.6) is necessary for satisfying the normalization (2.6).

Multiplying (3.5) by $\overline{\psi(\mathbf{x},t)}$, we find that the ODE (3.5) leaves $|\psi(\mathbf{x},t)|$ invariant in t [6, 7]. Hence, for $t \geq t_s$ (t_s is any given time), (3.5) becomes

$$i\,\frac{\partial\psi(\mathbf{x},t)}{\partial t} = \beta_d\,|\psi(\mathbf{x},t_s)|^2\psi(\mathbf{x},t),\ t \geq t_s, \qquad \mathbf{x}\in\mathbb{R}^d, \tag{3.7}$$

which can be integrated *exactly*, i.e.,

$$\psi(\mathbf{x},t) = e^{-i\beta_d|\psi(\mathbf{x},t_s)|^2(t-t_s)}\psi(\mathbf{x},t_s), \qquad t\geq t_s, \quad \mathbf{x}\in\mathbb{R}^d. \tag{3.8}$$

Thus, it remains to find an efficient and accurate scheme for (3.6). We shall construct below suitable spectral basis functions which are eigenfunctions of B so that $e^{-iB\Delta t}\psi$ can be exactly evaluated (which is necessary for the final scheme to be time reversible and time transverse invariant). Hence, the only time discretization error of the corresponding time-splitting method (3.2) is the splitting error, which is fourth order in Δt. Furthermore, the scheme is explicit, time reversible, and time transverse invariant, and as we shall show below, it also conserves the normalization in the discretized level.

3.1. Hermite pseudospectral method for the 1-D GPE. In the 1-D case, (3.6) collapses to

$$\begin{aligned} &i\,\frac{\partial\psi(z,t)}{\partial t} = B\psi(z,t) = -\frac{1}{2}\frac{\partial^2\psi(z,t)}{\partial z^2} + \frac{\gamma_z^2 z^2}{2}\psi(z,t), \quad z\in\mathbb{R},\\ &\lim_{|z|\to+\infty}\psi(z,t) = 0,\ t\geq 0, \end{aligned} \tag{3.9}$$

with the normalization (2.6)

$$\|\psi(\cdot,t)\|^2 = \int_{-\infty}^{\infty}|\psi(z,t)|^2dz \equiv \int_{-\infty}^{\infty}|\psi_0(z)|^2dz = 1. \tag{3.10}$$

Since the above equation is posed on the whole line, it is natural to consider Hermite functions which have been successfully applied to other equations (cf. [21, 25, 40]). Although the standard Hermite functions could be used as basis functions here, they are not the most appropriate. Below, we construct properly scaled Hermite functions which are eigenfunctions of B.

Let $H_l(z)$ $(l = 0, 1, \ldots, N)$ be the standard Hermite polynomials satisfying

$$H_l''(z) - 2zH_l'(z) + 2lH_l(z) = 0, \qquad z\in\mathbb{R}, \quad l\geq 0, \tag{3.11}$$

$$\int_{-\infty}^{\infty}H_l(z)H_n(z)e^{-z^2}\,dz = \sqrt{\pi}\,2^l\,l!\,\delta_{ln}, \qquad l,n\geq 0, \tag{3.12}$$

where δ_{ln} is the Kronecker delta. We define the scaled Hermite function

$$h_l(z) = e^{-\gamma_z z^2/2}\,H_l\left(\sqrt{\gamma_z}z\right)/\sqrt{2^l\,l!}(\pi/\gamma_z)^{1/4}, \qquad z\in\mathbb{R}. \tag{3.13}$$

Plugging (3.13) into (3.11) and (3.12), we find that

$$-\frac{1}{2}h_l''(z) + \frac{\gamma_z^2z^2}{2}h_l(z) = \mu_l^z h_l(z),\ z\in\mathbb{R}, \quad \mu_l^z = \frac{2l+1}{2}\gamma_z,\ l\geq 0, \tag{3.14}$$

$$\int_{-\infty}^{\infty}h_l(z)h_n(z)\,dz = \int_{-\infty}^{\infty}\frac{1}{\sqrt{\pi 2^l l!2^n n!}}H_l(z)H_n(z)e^{-z^2}\,dz = \delta_{ln},\ l,n\geq 0. \tag{3.15}$$

Hence, $\{h_l\}$ are eigenfunctions of B defined in (3.9).

For a fixed N, let $X_N = \mathrm{span}\{h_l : l = 0, 1, \ldots, N\}$. The Hermite spectral method for (3.9) is to find $\psi_N(z,t) \in X_N$, i.e.,

$$\psi_N(z,t) = \sum_{l=0}^{N} \hat{\psi}_l(t)\, h_l(z), \qquad z \in \mathbb{R}, \tag{3.16}$$

such that

$$i\,\frac{\partial \psi_N(z,t)}{\partial t} = B\psi_N(z,t) = -\frac{1}{2}\frac{\partial^2 \psi_N(z,t)}{\partial z^2} + \frac{\gamma_z^2 z^2}{2}\psi_N(z,t), \quad z \in \mathbb{R}. \tag{3.17}$$

Note that $\lim_{|z|\to+\infty} h_l(z) = 0$ (cf. [39]), so the decaying condition $\lim_{|z|\to+\infty} \psi_N(z,t) = 0$ is automatically satisfied.

Plugging (3.16) into (3.17), thanks to (3.14) and (3.15), we find

$$i\,\frac{d\hat{\psi}_l(t)}{dt} = \mu_l^z\ \hat{\psi}_l(t) = \frac{2l+1}{2}\gamma_z\ \hat{\psi}_l(t), \qquad l = 0, 1, \ldots, N. \tag{3.18}$$

Hence, the solution for (3.17) is given by

$$\psi_N(z,t) = e^{-iB(t-t_s)}\psi_N(z,t_s) = \sum_{l=0}^{N} e^{-i\mu_l^z (t-t_s)}\ \hat{\psi}_l(t_s) h_l(z), \qquad t \ge t_s. \tag{3.19}$$

Let $\{\hat{z}_k\}_{k=0}^N$ be the Hermite–Gauss points (cf. [39, 21]); i.e., $\{\hat{z}_k\}_{k=0}^N$ are the $N+1$ roots of the polynomial $H_{N+1}(z)$. Let ψ_k^n be the approximation of $\psi(z_k, t_n)$ and ψ^n be the solution vector with components ψ_k^n. Then, the fourth-order time-splitting Hermite pseudospectral (TSHP4) method for the 1-D GPE (2.5) is given by

$$\begin{aligned}
&\psi_k^{(1)} = e^{-i2w_1\ \Delta t\ \beta_1|\psi_k^n|^2}\ \psi_k^n, \qquad \psi_k^{(2)} = \mathcal{F}_h(w_2, \psi^{(1)})_k,\\
&\psi_k^{(3)} = e^{-i2w_3\ \Delta t\ \beta_1|\psi_k^{(2)}|^2}\ \psi_k^{(2)}, \qquad \psi_k^{(4)} = \mathcal{F}_h(w_4, \psi^{(3)})_k,\\
&\psi_k^{(5)} = e^{-i2w_3\ \Delta t\ \beta_1|\psi_k^{(4)}|^2}\ \psi_k^{(4)}, \qquad \psi_k^{(6)} = \mathcal{F}_h(w_2, \psi^{(5)})_k,\\
&\psi_k^{n+1} = e^{-i2w_1\ \Delta t\ \beta_1|\psi_k^{(6)}|^2}\ \psi_k^{(6)}, \qquad k = 0, 1, \ldots, N,
\end{aligned} \tag{3.20}$$

where w_i, $i = 1, 2, 3, 4$, are given in (3.3), and $\mathcal{F}_h(w, U)_k$ $(0 \le k \le N)$ can be computed from any given $w \in \mathbb{R}$ and $U = (U_0, \ldots, U_N)^T$:

$$\mathcal{F}_h(w,U)_k = \sum_{l=0}^{N} e^{-i2w\ \mu_l^z\ \Delta t}\ \widehat{U}_l\ h_l(z_k), \quad \widehat{U}_l = \sum_{k=0}^{N}\ \omega_k^z\ U(z_k)\ h_l(z_k). \tag{3.21}$$

In the above, z_k and ω_k^z are the scaled Hermite–Gauss points and weights, respectively, which are defined by

$$\omega_k^z = \frac{\hat{\omega}_k^z\ e^{\hat{z}_k^2}}{\sqrt{\gamma_z}}, \qquad z_k = \frac{\hat{z}_k}{\sqrt{\gamma_z}}, \qquad 0 \le k \le N, \tag{3.22}$$

where $\{\hat{\omega}_k^z\}_{k=0}^N$ are the weights associated with the Hermite–Gauss quadrature (cf. [21]) satisfying

$$\sum_{k=0}^{N}\ \hat{\omega}_k^z\ \frac{H_l(\hat{z}_k)}{\pi^{1/4}\sqrt{2^l\, l!}}\ \frac{H_n(\hat{z}_k)}{\pi^{1/4}\sqrt{2^n\, n!}} = \delta_{ln}, \qquad l, n = 0, 1, \ldots, N, \tag{3.23}$$

and we derive from (3.13) that

$$\sum_{k=0}^{N} \omega_k^z \, h_l(z_k) \, h_m(z_k) = \sum_{k=0}^{N} \hat{\omega}_k^z \, e^{\hat{z}_k^2/\sqrt{\gamma_z}} \, h_l\left(\hat{z}_k/\sqrt{\gamma_z}\right) \, h_m\left(\hat{z}_k/\sqrt{\gamma_z}\right)$$

$$= \sum_{k=0}^{N} \hat{\omega}_k^z \, \frac{H_l(\hat{z}_k)}{\pi^{1/4}\sqrt{2^l \, l!}} \, \frac{H_n(\hat{z}_k)}{\pi^{1/4}\sqrt{2^n \, n!}} = \delta_{ln}, \; 0 \le l, n \le N. \tag{3.24}$$

Note that the computation of $\{\omega_k^z\}$ from (3.22) is not a stable process for very large N. However, one can compute $\{\omega_k^z\}$ in a stable way as suggested in the appendix of [37].

Thus, the memory requirement of this scheme is $O(N)$, and the computational cost per time step is a small multiple of N^2. As for the stability of the TSHP4 method, we have the following.

LEMMA 3.1. *The TSHP4 method* (3.20) *is normalization conservation, i.e.,*

$$\|\psi^n\|_{l^2}^2 = \sum_{k=0}^{N} \omega_k^z |\psi_k^n|^2 = \sum_{k=0}^{M} \omega_k^z |\psi_0(z_k)|^2 = \|\psi_0\|_{l^2}^2, \qquad n = 0, 1, \ldots. \tag{3.25}$$

Proof. From (3.20), noting (3.21) and (3.24), we obtain

$$\begin{aligned}
\|\psi^{n+1}\|_{l^2}^2 &= \sum_{k=0}^{N} \omega_k^z |\psi_k^n|^2 = \sum_{k=0}^{N} \omega_k^z \left| e^{-i2w_1 \, \Delta t \, \beta_1 |\psi_k^{(6)}|^2} \, \psi_k^{(6)} \right|^2 \\
&= \sum_{k=0}^{N} \omega_k^z |\psi_k^{(6)}|^2 = \sum_{k=0}^{N} \omega_k^z \left| \sum_{l=0}^{N} e^{-i2w_2 \, \mu_l^z \, \Delta t} \, \widehat{(\psi^{(5)})}_l \, h_l(z_k) \right|^2 \\
&= \sum_{l=0}^{N} \sum_{m=0}^{N} e^{-i2w_2 \, \mu_l^z \, \Delta t} \, \widehat{(\psi^{(5)})}_l e^{i2w_2 \, \mu_m^z \, \Delta t} \, (\widehat{(\psi^{(5)})}_m)^* \left[\sum_{k=0}^{N} \omega_k^z h_l(z_k) h_m(z_k) \right] \\
&= \sum_{l=0}^{N} \sum_{m=0}^{N} e^{-i2w_2 \, \mu_l^z \, \Delta t} \, \widehat{(\psi^{(5)})}_l e^{i2w_2 \, \mu_m^z \, \Delta t} \, (\widehat{(\psi^{(5)})}_m)^* \, \delta_{lm} \\
&= \sum_{l=0}^{N} |\widehat{(\psi^{(5)})}_l|^2 = \sum_{l=0}^{N} \left| \sum_{k=0}^{N} \omega_k^z \, \psi^{(5)}(z_k) \, h_l(z_k) \right|^2 \\
&= \sum_{k=0}^{N} \sum_{m=0}^{N} \omega_k^z \psi^{(5)}(z_k) \psi^{(5)}(z_m)^* \left[\sum_{l=0}^{N} \omega_m^z h_l(z_k) h_l(z_m) \right] \\
&= \sum_{k=0}^{N} \sum_{m=0}^{N} \omega_k^z \psi^{(5)}(z_k) \psi^{(5)}(z_m)^* \, \delta_{km} \\
&= \sum_{k=0}^{N} \omega_k^z |\psi^{(5)}(z_k)|^2 = \|\psi^{(5)}\|_{l^2}^2.
\end{aligned} \tag{3.26}$$

Similarly, we have

$$\|\psi^{n+1}\|_{l^2}^2 = \|\psi^{(5)}\|_{l^2}^2 = \|\psi^{(3)}\|_{l^2}^2 = \|\psi^{(1)}\|_{l^2}^2 = \|\psi^n\|_{l^2}^2, \qquad n \ge 0. \tag{3.27}$$

Thus the equality (3.25) can be obtained from (3.27) by induction. ∎

Remark 3.2. Extension of the TSHP4 method (3.20) to the 2-D GPE without radial symmetry and the 3-D GPE without cylindrical symmetry is straightforward by using the tensor product of scaled Hermite functions.

3.2. Laguerre pseudospectral method for the 2-D GPE with radial symmetry. In the 2-D case with radial symmetry, i.e., $d = 2$ and $\gamma_x = \gamma_y$ in (2.5), and $\psi_0(x, y) = \psi_0(r)$ in (2.5) with $r = \sqrt{x^2 + y^2}$, we can write the solution of (2.5) as $\psi(x, y, t) = \psi(r, t)$. Therefore, (3.6) collapses to

$$\begin{aligned} & i\,\frac{\partial\psi(r,t)}{\partial t} = B\psi(r,t) = -\frac{1}{2r}\frac{\partial}{\partial r}\left(r\frac{\partial\psi(r,t)}{\partial r}\right) + \frac{\gamma_r^2 r^2}{2}\psi(r,t),\ 0 < r < \infty, \\ & \lim_{r\to\infty}\psi(r,t) = 0, \qquad t \ge 0, \end{aligned} \tag{3.28}$$

where $\gamma_r = \gamma_x = \gamma_y$. The normalization (2.6) collapses to

$$\|\psi(\cdot,t)\|^2 = 2\pi\int_0^\infty |\psi(r,t)|^2 r\,dr \equiv 2\pi\int_0^\infty |\psi_0(r)|^2 r\,dr = 1. \tag{3.29}$$

Note that it can be shown, similarly as for the Poisson equation in a 2-D disk (cf. [36]), that the problem (3.28) admits a unique solution without any condition at the pole $r = 0$.

Since (3.28) is posed on a semi-infinite interval, it is natural to consider Laguerre functions which have been successfully used for other problems in semi-infinite intervals (cf. [21, 37]). Again, the standard Laguerre functions, although usable, are not the most appropriate for this problem. Below, we construct properly scaled Laguerre functions which are eigenfunctions of B.

Let $\hat{L}_m(r)$ $(m = 0, 1, \ldots, M)$ be the Laguerre polynomials of degree m satisfying

$$r\hat{L}_m''(r) + (1 - r)\hat{L}_m'(r) + m\hat{L}_m(r) = 0, \qquad m = 0, 1, \ldots, \tag{3.30}$$

$$\int_0^\infty e^{-r}\,\hat{L}_m(r)\,\hat{L}_n(r)\,dr = \delta_{mn}, \qquad m, n = 0, 1, \ldots\ . \tag{3.31}$$

We define the scaled Laguerre functions L_m by

$$L_m(r) = \sqrt{\frac{\gamma_r}{\pi}}\,e^{-\gamma_r r^2/2}\,\hat{L}_m(\gamma_r r^2), \qquad 0 \le r < \infty. \tag{3.32}$$

Note that $\lim_{|r|\to+\infty} L_m(r) = 0$ (cf. [39]); hence, $\lim_{|r|\to+\infty}\psi_M(r,t) = 0$ is automatically satisfied.

Plugging (3.32) into (3.30) and (3.31), a simple computation shows

$$-\frac{1}{2r}\frac{\partial}{\partial r}\left(r\frac{\partial L_m(r)}{\partial r}\right) + \frac{1}{2}\gamma_r^2 r^2 L_m(r) = \mu_m^r L_m(r),\ \mu_m^r = \gamma_r(2m+1),\ m \ge 0, \tag{3.33}$$

$$2\pi\int_0^\infty L_m(r)L_n(r)r\,dr = \int_0^\infty e^{-r}\hat{L}_m(r)\hat{L}_n(r)\,dr = \delta_{mn},\ m, n \ge 0. \tag{3.34}$$

Hence, $\{L_m\}$ are eigenfunctions of B defined in (3.28).

For a fixed M, let $Y_M = \text{span}\{L_m : m = 0, 1, \ldots, M\}$. The Laguerre spectral method for (3.9) is to find $\psi_M(r, t) \in Y_M$, i.e.,

$$\psi_M(r,t) = \sum_{m=0}^{M}\hat{\psi}_m(t)\,L_m(r), \qquad 0 \le r < \infty, \tag{3.35}$$

such that

(3.36)
$$i\,\frac{\partial \psi_M(r,t)}{\partial t} = B\psi_M(r,t) = -\frac{1}{2r}\frac{\partial}{\partial r}\left(r\frac{\partial \psi_M(r,t)}{\partial r}\right) + \frac{\gamma_r^2 r^2}{2}\psi_M(r,t), \quad 0 < r < \infty.$$

Plugging (3.35) into (3.36), thanks to (3.33) and (3.34), we find

$$i\,\frac{d\hat{\psi}_m(t)}{dt} = \mu_m^r \hat{\psi}_m(t) = \gamma_z(2m+1)\hat{\psi}_m(t),\ m = 0, 1, \ldots, M. \tag{3.37}$$

Hence, the solution for (3.36) is given by

$$\psi_M(r,t) = e^{-iB(t-t_s)}\psi_M(r,t_s) = \sum_{m=0}^{M} e^{-i\mu_m^r(t-t_s)}\ \hat{\psi}_m(t_s)L_m(r), \qquad t \geq t_s. \tag{3.38}$$

Let $\{\hat{r}_j\}_{j=0}^M$ be the Laguerre–Gauss–Radau points (cf. [21]); i.e., they are the $M+1$ roots of the polynomial $r\hat{L}'_{M+1}(r)$. Let ψ_j^n be the approximation of $\psi(r_j, t_n)$ and ψ^n be the solution vector with components ψ_j^n. Then, the fourth-order time-splitting Laguerre pseudospectral (TSLP4) method for the 2-D GPE (2.5) with radial symmetry is similar to (3.20), except that one needs to replace β_1 by β_2, N by M, index k by j, and the operator $\mathcal{F}_h$ by $\mathcal{F}_L$, which is defined as

$$\mathcal{F}_L(w,U)_j = \sum_{l=0}^{M} e^{-i2w\ \mu_l^r\ \Delta t}\ \widehat{U}_l\ L_l(r_j), \quad \widehat{U}_l = \sum_{j=0}^{M} \omega_j^r\ U(r_j)\ L_l(r_j). \tag{3.39}$$

In the above, r_j and ω_j^r are the scaled Laguerre–Gauss–Radau points and weights, respectively, which are defined by

$$\omega_j^r = \frac{\pi}{\gamma_r}\ \hat{\omega}_j^r\ e^{\hat{r}_j}, \qquad r_j = \sqrt{\frac{\hat{r}_j}{\gamma_r}}, \qquad j = 0, 1, \ldots, M, \tag{3.40}$$

where $\{\hat{\omega}_j^r\}_{j=0}^M$ are the weights associated with the Laguerre–Gauss quadrature [21] satisfying

$$\sum_{j=0}^{M} \hat{\omega}_j^r \hat{L}_m(\hat{r}_j)\hat{L}_n(\hat{r}_j) = \delta_{nm}, \qquad n, m = 0, 1, \ldots, M,$$

and we derive from (3.32) that

$$\begin{aligned}\sum_{j=0}^{M} \omega_j^r L_m(r_j)L_n(r_j) &= \sum_{j=0}^{M} \hat{\omega}_j^r e^{\hat{r}_j}\pi/\gamma_r\ L_m\left(\sqrt{\hat{r}_j/\gamma_r}\right)\ L_n\left(\sqrt{\hat{r}_j/\gamma_r}\right)\\ &= \sum_{j=0}^{M} \hat{\omega}_j^r \hat{L}_m(\hat{r}_j)\hat{L}_n(\hat{r}_j) = \delta_{nm}, \quad n, m = 0, 1, \ldots, M.\end{aligned} \tag{3.41}$$

As in the Hermite case, the computation of $\{\omega_j^r\}$ from (3.40) is not a stable process for very large N. However, one can compute $\{\omega_j^r\}$ in a stable way as suggested in the appendix of [37].

The memory requirement of this scheme is $O(M)$, and the computational cost per time step is a small multiple of M^2. As for the stability of the TSLP4 method, we have the following.

LEMMA 3.3. *The TSLP4 method is normalization conservation, i.e.,*

$$\|\psi^n\|_{l^2}^2 = \sum_{j=0}^{M} \omega_j^r |\psi_j^n|^2 = \sum_{j=0}^{M} \omega_j^r |\psi_0(r_j)|^2 = \|\psi_0\|_{l^2}^2, \qquad n \geq 0.$$

Proof. Using (3.41), the proof is essentially the same as in Lemma 3.1 for the TSHP4 method. ∎

3.3. Laguerre–Hermite pseudospectral method for the 3-D GPE with cylindrical symmetry. In the 3-D case with cylindrical symmetry, i.e., $d = 3$ and $\gamma_x = \gamma_y$ in (2.5), and $\psi_0(x, y, z) = \psi_0(r, z)$ in (2.5), the solution of (2.5) with $d = 3$ satisfies $\psi(x, y, z, t) = \psi(r, z, t)$. Therefore, (3.6) becomes

$$\begin{aligned} i\,\frac{\partial \psi(r,z,t)}{\partial t} &= B\psi(r,z,t) = -\frac{1}{2}\left[\frac{1}{r}\frac{\partial}{\partial r}\left(r\frac{\partial \psi}{\partial r}\right) + \frac{\partial^2 \psi}{\partial z^2}\right] + \frac{1}{2}\left(\gamma_r^2 r^2 + \gamma_z^2 z^2\right)\psi, \\ & 0 < r < \infty,\ -\infty < z < \infty, \\ \lim_{r\to\infty} \psi(r,z,t) = 0, &\quad \lim_{|z|\to\infty} \psi(r,z,t) = 0, \qquad t \geq 0, \end{aligned} \tag{3.42}$$

where $\gamma_r = \gamma_x = \gamma_y$. The normalization (2.6) becomes

$$\|\psi(\cdot,t)\|^2 = 2\pi \int_0^\infty \int_{-\infty}^\infty |\psi(r,z,t)|^2 r\, dr dz \equiv \|\psi_0\|^2 = 1. \tag{3.43}$$

We are now in position to present our Laguerre–Hermite pseudospectral method for (3.42).

Using the same notation as in previous subsections, we derive from (3.14) and (3.33) that

$$\begin{aligned} &-\frac{1}{2}\left[\frac{1}{r}\frac{\partial}{\partial r}\left(r\frac{\partial}{\partial r}\right) + \frac{\partial^2}{\partial z^2}\right](L_m(r)\, h_l(z)) + \frac{1}{2}\left(\gamma_r^2 r^2 + \gamma_z^2 z^2\right)(L_m(r)\, h_l(z)) \\ &= \left[-\frac{1}{2r}\frac{d}{dr}\left(r\frac{dL_m(r)}{dr}\right) + \frac{1}{2}\gamma_r^2 r^2 L_m(r)\right] h_l(z) + \left[-\frac{1}{2}\frac{d^2 h_l(z)}{dz^2} + \frac{1}{2}\gamma_z^2 z^2 h_l(z)\right] L_m(r) \\ &= \mu_m^r L_m(r) h_l(z) + \mu_l^z h_l(z) L_m(r) = (\mu_m^r + \mu_l^z) L_m(r) h_l(z). \end{aligned} \tag{3.44}$$

Hence, $\{L_m(r)h_l(z)\}$ are eigenfunctions of B defined in (3.42).

For a fixed pair (M, N), let $X_{MN} = \text{span}\{L_m(r)h_l(z) : m = 0, 1, \ldots, M,\ l = 0, 1, \ldots, N\}$. The Laguerre–Hermite spectral method for (3.42) is to find $\psi_{MN}(r, z, t) \in X_{MN}$, i.e.,

$$\psi_{MN}(r,z,t) = \sum_{m=0}^{M}\sum_{l=0}^{N} \tilde{\psi}_{ml}(t)\, L_m(r)\, h_l(z), \tag{3.45}$$

such that

$$\begin{aligned} i\,\frac{\partial \psi_{MN}(r,z,t)}{\partial t} &= B\psi_{MN}(r,z,t) \\ &= -\frac{1}{2}\left[\frac{1}{r}\frac{\partial}{\partial r}\left(r\frac{\partial \psi_{MN}}{\partial r}\right) + \frac{\partial^2 \psi_{MN}}{\partial z^2}\right] + \frac{1}{2}\left(\gamma_r^2 r^2 + \gamma_z^2 z^2\right)\psi_{MN}. \end{aligned} \tag{3.46}$$

Plugging (3.45) into (3.46), thanks to (3.44), we find that

$$i\,\frac{d\tilde{\psi}_{ml}(t)}{dt} = (\mu_m^r + \mu_l^z)\,\tilde{\psi}_{ml}(t),\ m = 0, 1, \ldots, M,\ l = 0, 1, \ldots, N. \tag{3.47}$$

Hence, the solution for (3.46) is given by

$$\begin{aligned}\psi_{MN}(r, z, t) &= e^{-iB(t-t_s)}\psi_{MN}(r, z, t_s)\\ &= \sum_{m=0}^{M}\sum_{l=0}^{N} e^{-i(\mu_m^r+\mu_l^z)(t-t_s)}\tilde{\psi}_{ml}(t_s)L_m(r)\,h_l(z), \qquad t \ge t_s.\end{aligned} \tag{3.48}$$

Let ψ_{jk}^n be the approximation of $\psi(r_j, z_k, t_n)$ and ψ^n be the solution vector with components ψ_{jk}^n. The fourth-order time-splitting Laguerre–Hermite pseudospectral (TSLHP4) method for the 3-D GPE (2.5) with cylindrical symmetry is similar to (3.20), except that we replace β_1 by β_3, index k $(0 \le k \le N)$ by jk $(0 \le j \le M,$ $0 \le k \le N)$, and the operator $\mathcal{F}_h$ by $\mathcal{F}_{Lh}$, which is defined as

$$\begin{aligned}\mathcal{F}_{Lh}(w, U)_{jk} &= \sum_{m=0}^{M}\sum_{l=0}^{N} e^{-i2w\Delta t(\mu_m^r+\mu_l^z)}\,\widehat{U}_{ml}\,L_m(r_j)h_l(z_k),\\ \widehat{U}_{ml} &= \sum_{j=0}^{M}\sum_{k=0}^{N}\omega_j^r\,\omega_k^z\,U(r_j, z_k)\,L_m(r_j)h_l(z_k).\end{aligned} \tag{3.49}$$

The memory requirement of this scheme is $O(MN)$, and the computational cost per time step is $O(\max(M^2N, N^2M))$. As for the stability of the TSLHP4 method, we have the following.

LEMMA 3.4. *The TSLHP4 method is normalization conservation, i.e.,*

$$\|\psi^n\|_{l^2}^2 = \sum_{j=0}^{M}\sum_{k=0}^{N}\omega_j^r\omega_k^z|\psi_{jk}^n|^2 = \sum_{j=0}^{M}\sum_{k=0}^{N}\omega_j^r\omega_k^z|\psi_0(r_j, z_k)|^2 = \|\psi_0\|_{l^2}^2, \quad n \ge 0.$$

Proof. Using (3.24) and (3.41), the proof is essentially the same as in Lemma 3.1 for the TSHP4 method. ∎

4. Extension to multicomponent BECs. The TSLHP4 method, introduced above for the 3-D GPE with cylindrical symmetry, can be extended to VGPEs for multicomponent BECs [4]. For simplicity, we present only the detailed method for the dynamics of two-component BECs. Consider the dimensionless VGPEs with an external driven field (cf. [4])

$$\begin{aligned}i\,\frac{\partial\psi(r, z, t)}{\partial t} &= -\frac{1}{2}\left[\frac{1}{r}\frac{\partial}{\partial r}\left(r\frac{\partial\psi}{\partial r}\right) + \frac{\partial^2\psi}{\partial z^2}\right] + \frac{1}{2}\left(\gamma_r^2r^2 + \gamma_z^2(z - z_1^0)^2\right)\psi\\ &\quad + \left(\beta_{11}|\psi|^2 + \beta_{12}|\phi|^2\right)\psi + \sqrt{N_2^0/N_1^0}f(t)\phi,\\ i\,\frac{\partial\phi(r, z, t)}{\partial t} &= -\frac{1}{2}\left[\frac{1}{r}\frac{\partial}{\partial r}\left(r\frac{\partial\phi}{\partial r}\right) + \frac{\partial^2\phi}{\partial z^2}\right] + \frac{1}{2}\left(\gamma_r^2r^2 + \gamma_z^2(z - z_2^0)^2\right)\phi\\ &\quad + \left(\beta_{21}|\psi|^2 + \beta_{22}|\phi|^2\right)\phi + \sqrt{N_1^0/N_2^0}f(t)\psi,\ 0 < r < \infty,\ z \in \mathbb{R},\\ \lim_{r\to\infty}\psi(r, z, t) &= \lim_{r\to\infty}\phi(r, z, t) = 0,\ \lim_{|z|\to\infty}\psi(r, z, t) = \lim_{|z|\to\infty}\phi(r, z, t) = 0,\\ \psi(r, z, 0) &= \psi_0(r, z), \qquad \phi(r, z, 0) = \phi_0(r, z),\end{aligned} \tag{4.1}$$

where z_j^0 and N_j^0 $(j = 1, 2)$ are the center of trapping potential along the z-axis and the number of atoms of the jth component, respectively; $\gamma_r = \omega_r/\omega_m$, $\gamma_z = \omega_z/\omega_m$, with ω_r, ω_z, and ω_m being the radial, axial, and reference frequencies, respectively; $\beta_{jl} = 4\pi a_{jl} N_l^0/a_0$ $(j, l = 1, 2)$, with the s-wave scattering length $a_{jl} = a_{lj}$ between the jth and lth component and $a_0 = \sqrt{\hbar/m\omega_m}$; and $f(t) = \Omega\cos(\omega_d t/\omega_m)/\omega_m$, with Ω and ω_d being the amplitude and frequency of the external driven field. The wave functions are normalized as

$$\|\psi_0\|^2 = 2\pi \int_0^\infty \int_{-\infty}^\infty |\psi_0(r,z)|^2 r\, dr dz = 1, \quad \|\phi_0\|^2 = 1. \tag{4.2}$$

It is easy to show (cf. [4]) that the total number of atoms is conserved:

$$\begin{aligned} N_1^0\|\psi(\cdot,t)\|^2 + N_2^0\|\phi(\cdot,t)\|^2 &= 2\pi \int_0^\infty \int_{-\infty}^\infty \left(|\psi(r,z,t)|^2 + |\phi(r,z,t)|^2\right) r\, dr dz \\ &\equiv N_1^0\|\psi_0\|^2 + N_2^0\|\phi_0\|^2 = N_1^0 + N_2^0. \end{aligned} \tag{4.3}$$

Unlike the TSLHP4 method for the 3-D GPE (2.5) with cylindrical symmetry, here we have to split the VGPEs (4.1) into three subsystems. For example, for a first-order splitting scheme, we first solve

$$\begin{aligned} i\,\frac{\partial\psi(r,z,t)}{\partial t} &= -\frac{1}{2}\left[\frac{1}{r}\frac{\partial}{\partial r}\left(r\frac{\partial\psi}{\partial r}\right) + \frac{\partial^2\psi}{\partial z^2}\right] + \frac{1}{2}\left(\gamma_r^2 r^2 + \gamma_z^2 z^2\right)\psi, \\ i\,\frac{\partial\phi(r,z,t)}{\partial t} &= -\frac{1}{2}\left[\frac{1}{r}\frac{\partial}{\partial r}\left(r\frac{\partial\phi}{\partial r}\right) + \frac{\partial^2\phi}{\partial z^2}\right] + \frac{1}{2}\left(\gamma_r^2 r^2 + \gamma_z^2 z^2\right)\phi \end{aligned} \tag{4.4}$$

for the time step of length Δt, followed by solving

$$\begin{aligned} i\,\frac{\partial\psi(r,z,t)}{\partial t} &= \frac{1}{2}\gamma_z^2 z_1^0(z_1^0 - 2z)\psi + \left(\beta_{11}|\psi|^2 + \beta_{12}|\phi|^2\right)\psi, \\ i\,\frac{\partial\phi(r,z,t)}{\partial t} &= \frac{1}{2}\gamma_z^2 z_2^0(z_2^0 - 2z)\phi + \left(\beta_{21}|\psi|^2 + \beta_{22}|\phi|^2\right)\phi \end{aligned} \tag{4.5}$$

for the same time step, and then by solving

$$\begin{aligned} i\,\frac{\partial\psi(r,z,t)}{\partial t} &= \sqrt{N_2^0/N_1^0}\, f(t)\,\phi, \\ i\,\frac{\partial\phi(r,z,t)}{\partial t} &= \sqrt{N_1^0/N_2^0}\, f(t)\,\psi \end{aligned} \tag{4.6}$$

for the same time step.

The nonlinear ODE system (4.5) leaves $|\psi(r,z,t)|$ and $|\phi(r,z,t)|$ invariant in t, and thus can be integrated *exactly* [4]. The linear ODE system (4.6) can also be integrated *exactly* by applying a matrix diagonalization technique (cf. [4]). As shown above, (4.4) can be discretized in space by the Laguerre–Hermite pseudospectral method and integrated in time *exactly*.

Let ψ_{jk}^n and ϕ_{jk}^n be the approximations of $\psi(r_j, z_k, t_n)$ and $\phi(r_j, z_k, t_n)$, respectively, and ψ^n and ϕ^n be the solution vectors with components ψ_{jk}^n and ϕ_{jk}^n, respectively. Although it is not clear how to construct a fourth-order time-splitting scheme with three subsystems, a second-order scheme can be easily constructed using the

Strang splitting (cf. [38]). More precisely, from time $t = t_n$ to $t = t_{n+1}$, we proceed as follows:

$$
\begin{aligned}
&\psi_{jk}^{(1)} = \mathcal{F}_{Lh}(1/4, \psi^{(1)})_{jk}, \qquad \phi_{jk}^{(1)} = \mathcal{F}_{Lh}(1/4, \phi^{(1)})_{jk},\\
&\psi_{jk}^{(2)} = e^{-i[\gamma_z^2 z_1^0 (z_1^0 - 2z_k)/2 + (\beta_{11}|\psi_{jk}^{(1)}|^2 + \beta_{12}|\phi_{jk}^{(1)}|^2)]\Delta t/2} \psi_{jk}^{(1)},\\
&\phi_{jk}^{(2)} = e^{-i[\gamma_z^2 z_2^0 (z_2^0 - 2z_k)/2 + (\beta_{21}|\psi_{jk}^{(1)}|^2 + \beta_{22}|\phi_{jk}^{(1)}|^2)]\Delta t/2} \phi_{jk}^{(1)},\\
&\psi_{jk}^{(3)} = \cos(g(t_{n+1}, t_n))\psi_{jk}^{(2)} - i\sin(g(t_{n+1}, t_n))\sqrt{N_2^0/N_1^0}\phi_{jk}^{(2)},\\
&\phi_{jk}^{(3)} = -i\sin(g(t_{n+1}, t_n))\sqrt{N_1^0/N_2^0}\psi_{jk}^{(2)} + \cos(g(t_{n+1}, t_n))\phi_{jk}^{(2)},\\
&\psi_{jk}^{(4)} = e^{-i[\gamma_z^2 z_1^0 (z_1^0 - 2)/2 + (\beta_{11}|\psi_{jk}^{(3)}|^2 + \beta_{12}|\phi_{jk}^{(3)}|^2)]\Delta t/2} \psi_{jk}^{(3)},\\
&\phi_{jk}^{(4)} = e^{-i[\gamma_z^2 z_2^0 (z_2^0 - 2)/2 + (\beta_{21}|\psi_{jk}^{(3)}|^2 + \beta_{22}|\phi_{jk}^{(3)}|^2)]\Delta t/2} \phi_{jk}^{(3)}, \quad 0 \le j \le M,\ 0 \le k \le N,\\
&\psi_{jk}^{n+1} = \mathcal{F}_{Lh}(1/4, \psi^{(4)})_{jk}, \qquad \phi_{jk}^{n+1} = \mathcal{F}_{Lh}(1/4, \phi^{(4)})_{jk},
\end{aligned}
\tag{4.7}
$$

where

$$
g(t, t_n) = \int_{t_n}^{t} f(s)\, ds = \Omega\omega_d \left[\sin(\omega_d t/\omega_m) - \sin(\omega_d t_n/\omega_m)\right].
$$

Note that the only time discretization error of this scheme is the splitting error, which is of second order in Δt. The scheme is explicit, spectral accurate in space, and second-order accurate in time. The memory requirement of this method is $O(MN)$, and the computational cost per time step is $O(\max(M^2N, MN^2))$. As for the stability, we can prove as in [4] the following lemma, which shows that the total number of atoms is conserved in the discretized level.

LEMMA 4.1. *The time-splitting Laguerre–Hermite pseudospectral method* (4.7) *for multicomponent BECs is normalization conservation, i.e.,*

$$
N_1^0\|\psi^n\|_{l^2}^2 + N_2^0\|\phi^n\|_{l^2}^2 = N_1^0\|\psi_0\|_{l^2}^2 + N_2^0\|\phi_0\|_{l^2}^2, \quad n \ge 0.
$$

5. Numerical results. We now present some numerical results by using the numerical methods introduced in section 3. To quantify the numerical results, we define the condensate width along the r- and z-axes as

$$
\sigma_\alpha^2 = \int_{\mathbb{R}^d} \alpha^2 |\psi(\mathbf{x}, t)|\, d\mathbf{x}, \quad \alpha = x, y, z, \qquad \sigma_r^2 = \sigma_x^2 + \sigma_y^2.
$$

Example 5.1. The 1-D GPE: We choose $d = 1$, $\gamma_z = 2$, and $\beta_1 = 50$ in (2.5). The initial data $\psi_0(z)$ is chosen as the ground state of the 1-D GPE (2.5) with $d = 1$, $\gamma_z = 1$, and $\beta_1 = 50$ [5, 8]. This corresponds to an experimental setup where initially the condensate is assumed to be in its ground state, and the trap frequency is double at $t = 0$. We solve this problem by using (3.20) with $N = 31$ and time step $k = 0.001$. Figure 5.1 plots the condensate width and central density $|\psi(0, t)|^2$ as functions of time. Our numerical experiments also show that the scheme (3.20) with $N = 31$ gives similar numerical results as the TSSP method [9, 10] for this example with 129 grid points over the interval $[-12, 12]$ and time step $k = 0.001$.

In order to test the fourth-order accuracy in time of the TSHP4 method (3.20), we compute a numerical solution with a very fine mesh, e.g., $N = 81$, and a very small

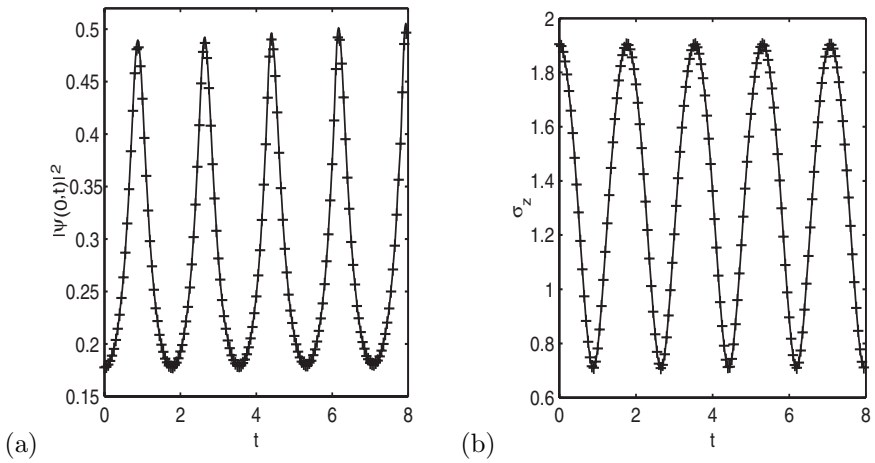

(a) (b)

FIG. 5.1. *Evolution of central density and condensate width in Example* 5.1. *"—": "exact solutions" obtained by the TSSP method* [9] *with* 513 *grid points over an interval* $[-12, 12]$*; "+ + +": Numerical results by the TSHP4 method* (3.20) *with* 31 *grid points on the whole z-axis.* (a) *Central density* $|\psi(0,t)|^2$*;* (b) *condensate width* σ_z.

TABLE 5.1
Time discretization error analysis for the TSHP4 method (3.20) *at* $t = 2.0$ *with* $N = 81$.

Δt	1/40	1/80	1/160	1/320
$\max\|\psi(t) - \psi^{\Delta t}(t)\|$	0.1619	4.715E-6	3.180E-7	2.036E-8
$\|\psi(t) - \psi^{\Delta t}(t)\|_{l^2}$	0.2289	7.379E-6	4.925E-7	3.215E-8

time step, e.g., $\Delta t = 0.0001$, as the "exact" solution ψ. Let $\psi^{\Delta t}$ denote the numerical solution under $N = 81$ and time step Δt. Due to N being large enough, the truncation error from space discretization is negligible compared to that from time discretization. Table 5.1 shows the errors $\max|\psi(t) - \psi^{\Delta t}(t)|$ and $\|\psi(t) - \psi^{\Delta t}(t)\|_{l^2}$ at $t = 2.0$ for different time step Δt. The results in Table 5.1 demonstrate the fourth-order accuracy in time of the TSHP4 method (3.20).

Example 5.2. The 2-D GPE with radial symmetry: We choose $d = 2$, $\gamma_r = \gamma_x = \gamma_y = 2$, and $\beta_2 = 50$ in (2.5). The initial data $\psi_0(r)$ is chosen as the ground state of the 2-D GPE (2.5) with $d = 2$, $\gamma_r = \gamma_x = \gamma_y = 1$, and $\beta_2 = 50$ [5, 8]. Again this corresponds to an experimental setup where initially the condensate is assumed to be in its ground state, and the trap frequency is doubled at $t = 0$. We solve this problem by using the TSLP4 method with $M = 30$ and time step $k = 0.001$. Figure 5.2 plots the condensate width and central density $|\psi(0,t)|^2$ as functions of time. Our numerical experiments also show that the scheme TSLP4 method with $M = 30$ gives similar numerical results as the TSSP method [9, 10] for this example with 129^2 grid points over the box $[-8, 8]^2$ and time step $k = 0.001$.

Example 5.3. The 3-D GPE with cylindrical symmetry: We choose $d = 3$, $\gamma_r = \gamma_x = \gamma_y = 4$, $\gamma_z = 1$, and $\beta_3 = 100$ in (2.5). The initial data $\psi_0(r, z)$ is chosen as the ground state of the 3-D GPE (2.5) with $d = 3$, $\gamma_r = \gamma_x = \gamma_y = 1$, $\gamma_z = 4$, and $\beta_3 = 100$ [5, 8]. This corresponds to an experimental setup where initially the condensate is assumed to be in its ground state, and at $t = 0$ we increase the radial frequency four times and decrease the axial frequency to its quarter. We solve this problem by using the TSLP4 method with $M = 60$ and $N = 61$ and time step

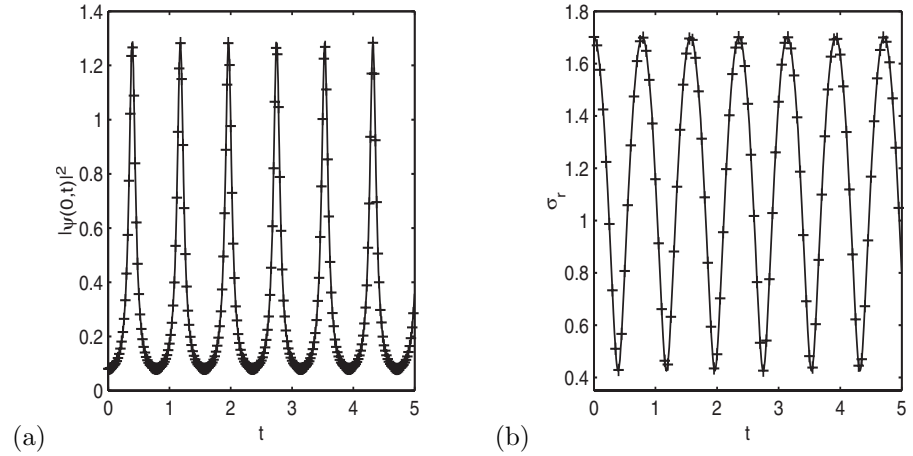

FIG. 5.2. *Evolution of central density and condensate width in Example* 5.2. *"—": "exact solutions" obtained by the TSSP method* [9] *with* 513^2 *grid points over a box* $[-8,8]^2$*; "+ + +": Numerical results by the TSLP4 method with* 30 *grid points on the semi-infinite interval* $[0,\infty)$. (a) *Central density* $|\psi(0,t)|^2$*;* (b) *condensate width* σ_r.

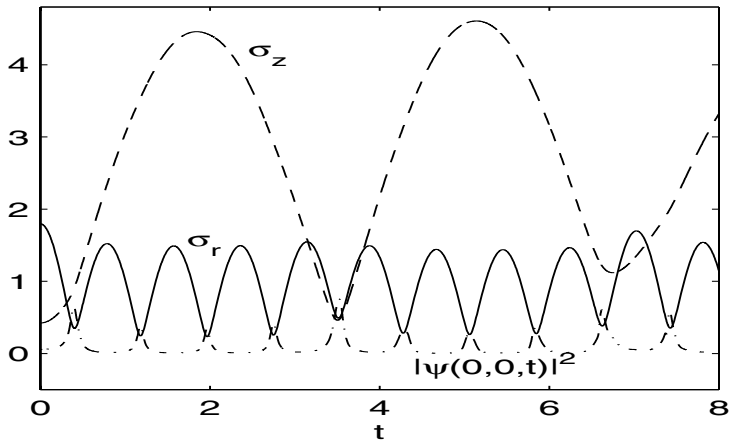

FIG. 5.3. *Evolution of central density and condensate width in Example* 5.3 *by the TSLHP4 method.*

$k = 0.001$. Figure 5.3 plots the condensate widths and central density $|\psi(0,0,t)|^2$ as functions of time.

The numerical results for these three examples clearly indicated that our new methods are very efficient and accurate.

Example 5.4. The 3-D vector GPEs with cylindrical symmetry for two-component BECs: We take, in (4.1), $m = 1.44 \times 10^{-25}$ $[kg]$, $a_{12} = a_{21} = 55.3\text{Å} = 5.53$ $[nm]$, $a_{11} = 1.03a_{12} = 5.6959$ $[nm]$, $a_{22} = 0.97a_{12} = 5.3641$ $[nm]$, $\omega_z = 47 \times 2\pi$ $[1/s]$, $\omega_m = \omega_r = \omega_z/\sqrt{8}$, $N_1^0 = N_2^0 = 500,000$, $\Omega = 65 \times 2\pi$ $[1/s]$, and $\omega_d = 6.5 \times 2\pi$ $[1/s]$. A simple computation shows $a_0 = 0.2643 \times 10^{-5}$ $[m]$, $\beta_{11} = 0.02708165N_1^0$, $\beta_{12} = 0.02629286N_2^0$, $\beta_{21} = 0.02629286N_1^0$, and $\beta_{22} = 0.02550407N_2^0$. The initial data $\psi_0(r,z)$ and $\phi_0(r,z)$ are chosen as the ground state of the 3-D VGPEs (4.1), and we

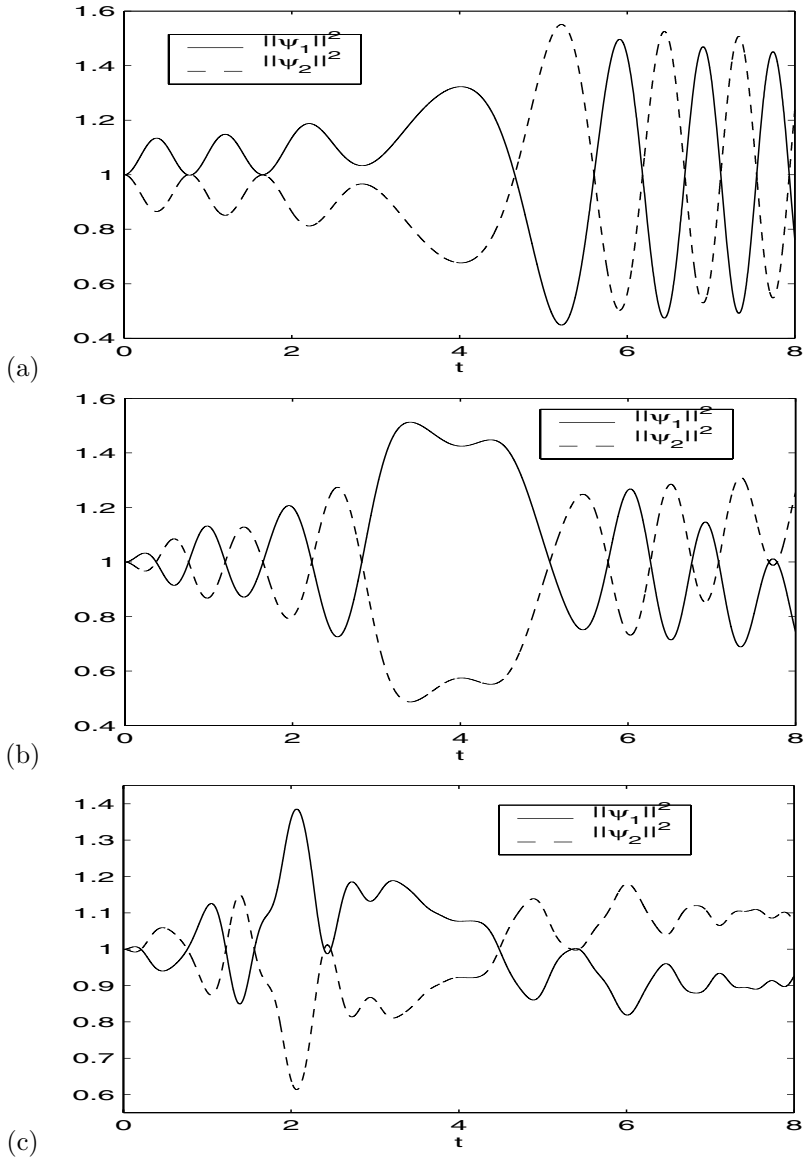

FIG. 5.4. *Time evolution of the density functions for the two-component BECs in Example* 5.4. (a) $z_1^0 = z_2^0 = 0$; (b) $z_1^0 = -z_2^0 = 0.15$; (c) $z_1^0 = -z_2^0 = 0.4$.

set $f(t) \equiv 0$ [4]. We solve this problem by using (4.7) with $M = 100$ and $N = 201$ and time step $k = 0.00025$. Figure 5.4 displays the time evolution of the density functions for the two components with different trapping centers. The results are similar to those obtained in [4] by a TSSP method with a much refined grid.

From Figure 5.4, we can see that the general form of time evolution on the number of particles in the two components is similar for different distances between the two trapping potential centers. When $z_1^0 = z_2^0 = 0$, the number of particles in the second component, i.e., $N_2^0\|\phi\|^2$, decreases, reaching its bottom, oscillates, and then attains its maximum at around $t = 5.2$. The number of particles in the second component

at its maximum is approximately 55% bigger than its initial value at time $t = 0$ (cf. Figure 5.4(a)). The pattern for $N_1^0\|\psi\|^2$ is exactly the opposite of that for $N_2^0\|\phi\|^2$ (cf. Figure 5.4(a)). This antisymmetry is due to the fact that the total number of particles in the two components are conserved. When $z_1^0 - z_2^0 > 0$ becomes larger, i.e., initially the density functions for the two components are separated further, the earlier the number of particles attains its absolute peak (cf. Figure 5.4(b–c)) and the smaller the maximum of the peak. In fact, when $z_1^0 - z_2^0 = 0.3$ (resp., 0.8), at around $t = 3.4$ (resp., 2.05), the number of particles in the first component attains its maximum which is approximately 52% (resp., 38.5%) bigger than its initial value at time $t = 0$.

6. Concluding remarks. We developed a new efficient fourth-order time-splitting Laguerre–Hermite pseudospectral method for the 3-D GPE with cylindrical symmetry for BECs. The new method takes advantage of the cylindrical symmetry so that only an effective 2-D problem is solved numerically. The new method is based on appropriately scaled Laguerre–Hermite functions and a fourth-order symplectic integrator. Hence, it is spectrally accurate in space, fourth-order accurate in time, explicit, time reversible, and time transverse invariant.

When compared with the time-splitting sine-spectral method in [9, 10, 4] and the CNFD method in [34, 31], the new method enjoys two important advantages: (i) there is no need to truncate the original whole space into a bounded computational domain for which an artificial boundary condition (which often erodes the accuracy) is needed; (ii) it solves an effective 2-D problem instead of the original 3-D equations. Thus, the new method is very accurate and efficient, particularly in terms of memory requirement. Therefore, it is extremely suitable for the 3-D GPE with cylindrical symmetry, which is the most frequent setup in BEC experiments. We plan to apply this powerful numerical method to study physically more complex systems such as multicomponent BECs, vortex states, and dynamics in BECs.

REFERENCES

[1] A. Aftalion and Q. Du, *Vortices in a rotating Bose-Einstein condensate: Critical angular velocities and energy diagrams in the Thomas-Fermi regime*, Phys. Rev. A, 64 (2001), 063603.

[2] M. H. Anderson, J. R. Ensher, M. R. Matthews, C. E. Wieman, and E. A. Cornell, *Observation of Bose-Einstein condensation in a dilute atomic vapor*, Science, 269 (1995), pp. 198–201.

[3] J. R. Anglin and W. Ketterle, *Bose-Einstein condensation of atomic gases*, Nature, 416 (2002), pp. 211–218.

[4] W. Bao, *Ground states and dynamics of multicomponent Bose–Einstein condensates*, Multiscale Model. Simul., 2 (2004), pp. 210–236.

[5] W. Bao and Q. Du, *Computing the ground state solution of Bose–Einstein condensates by a normalized gradient flow*, SIAM J. Sci. Comput., 25 (2004), pp. 1674–1697.

[6] W. Bao, S. Jin, and P. A. Markowich, *On time-splitting spectral approximations for the Schrödinger equation in the semiclassical regime*, J. Comput. Phys., 175 (2002), pp. 487–524.

[7] W. Bao, S. Jin, and P. A. Markowich, *Numerical study of time-splitting spectral discretizations of nonlinear Schrödinger equations in the semiclassical regimes*, SIAM J. Sci. Comput., 25 (2003), pp. 27–64.

[8] W. Bao and W. Tang, *Ground-state solution of Bose-Einstein condensate by directly minimizing the energy functional*, J. Comput. Phys., 187 (2003), pp. 230–254.

[9] W. Bao, D. Jaksch, and P. A. Markowich, *Numerical solution of the Gross-Pitaevskii equation for Bose-Einstein condensation*, J. Comput. Phys., 187 (2003), pp. 318–342.

[10] W. Bao and D. Jaksch, *An explicit unconditionally stable numerical method for solving damped nonlinear Schrodinger equations with a focusing nonlinearity*, SIAM J. Numer. Anal., 41 (2003), pp. 1406–1426.

[11] G. Baym and C. J. Pethick, *Ground-state properties of magnetically trapped Bose-condensed rubidium gas*, Phys. Rev. Lett., 76 (1996), pp. 6–9.
[12] C. C. Bradley, C. A. Sackett, and R. G. Hulet, *Bose-Einstein condensation of lithium: Observation of limited condensate number*, Phys. Rev. Lett., 78 (1997), pp. 985–989.
[13] M. M. Cerimele, M. L. Chiofalo, F. Pistella, S. Succi, and M. P. Tosi, *Numerical solution of the Gross-Pitaevskii equation using an explicit finite-difference scheme: An application to trapped Bose-Einstein condensates*, Phys. Rev. E, 62 (2000), pp. 1382–1389.
[14] M. M. Cerimele, F. Pistella, and S. Succi, *Particle-inspired scheme for the Gross-Pitaevskii equation: An application to Bose-Einstein condensation*, Comput. Phys. Comm., 129 (2000), pp. 82–90.
[15] M. L. Chiofalo, S. Succi, and M. P. Tosi, *Ground state of trapped interacting Bose-Einstein condensates by an explicit imaginary-time algorithm*, Phys. Rev. E, 62 (2000), pp. 7438–7444.
[16] E. Cornell, *Very cold indeed: The nanokelvin physics of Bose-Einstein condensation*, J. Res. Natl. Inst. Stan., 101 (1996), pp. 419–434.
[17] F. Dalfovo, S. Giorgini, L. P. Pitaevskii, and S. Stringari, *Theory of Bose-Einstein condensation in trapped gases*, Rev. Modern Phys., 71 (1999), pp. 463–512.
[18] R. J. Dodd, *Approximate solutions of the nonlinear Schrödinger equation for ground and excited states of Bose-Einstein condensates*, J. Res. Natl. Inst. Stan., 101 (1996), pp. 545–552.
[19] M. Edwards and K. Burnett, *Numerical solution of the nonlinear Schrödinger equation for small samples of trapped neutral atoms*, Phys. Rev. A, 51 (1995), pp. 1382–1386.
[20] M. Edwards, P. A. Ruprecht, K. Burnett, R. J. Dodd, and C. W. Clark, *Collective excitations of atomic Bose-Einstein condensates*, Phys. Rev. Lett., 77 (1996), pp. 1671–1674.
[21] D. Funaro, *Polynomial Approximations of Differential Equations*, Springer-Verlag, Berlin, 1992.
[22] M. Greiner, O. Mandel, T. Esslinger, T. W. Hänsch, and I. Bloch, *Quantum phase transition from a superfluid to a mott insulator in a gas of ultracold atoms*, Nature, 415 (2002), pp. 39–45.
[23] A. Griffin, D. Snoke, and S. Stringari, eds., *Bose-Einstein Condensation*, Cambridge University Press, New York, 1995.
[24] E. P. Gross, *Structure of a quantized vortex in boson systems*, Nuovo Cimento (10), 20 (1961), pp. 454–477.
[25] B.-Y. Guo, J. Shen, and C.-L. Xu, *Spectral and pseudospectral approximations using Hermite functions: Application to the Dirac equation*, Adv. Comput. Math., 19 (2003), pp. 35–55.
[26] D. S. Hall, M. R. Matthews, J. R. Ensher, C. E. Wieman, and E. A. Cornell, *Dynamics of component separation in a binary mixture of Bose-Einstein condensates*, Phys. Rev. Lett., 81 (1998), pp. 1539–1542.
[27] D. Jaksch, C. Bruder, J. I. Cirac, C. W. Gardiner, and P. Zoller, *Cold bosonic atoms in optical lattices*, Phys. Rev. Lett., 81 (1998), pp. 3108–3111.
[28] L. Laudau and E. Lifschitz, *Quantum Mechanics: Non-Relativistic Theory*, Pergamon Press, New York, 1977.
[29] P. Leboeuf and N. Pavloff, *Bose-Einstein beams: Coherent propagation through a guide*, Phys. Rev. A, 64 (2001), 033602.
[30] J. Lee and B. Fornberg, *A split step approach for the* 3*-d Maxwell's equations*, J. Comput. Appl. Math., 158 (2003), pp. 485–505.
[31] P. Muruganandam and S. K. Adhikari, *Bose-Einstein condensation dynamics in three dimensions by the pseudospectral and finite-difference methods*, J. Phys. B: At. Mol. Opt. Phys., 36 (2003), pp. 2501–2513.
[32] L. P. Pitaevskii, *Vortex lines in an imperfect Bose gas*, Zh. Eksp. Teor. Fiz., 40 (1961), pp. 646–649 (in Russian); Sov. Phys. JETP, 13 (1961), pp. 451–454 (in English).
[33] D. S. Rokhsar, *Vortex stability and persistent currents in trapped Bose gas*, Phys. Rev. Lett., 79 (1997), pp. 2164–2167.
[34] P. A. Ruprecht, M. J. Holland, K. Burrett, and M. Edwards, *Time-dependent solution of the nonlinear Schrödinger equation for Bose-condensed trapped neutral atoms*, Phys. Rev. A, 51 (1995), pp. 4704–4711.
[35] B. I. Schneider and D. L. Feder, *Numerical approach to the ground and excited states of a Bose-Einstein condensated gas confined in a completely anisotropic trap*, Phys. Rev. A, 59 (1999), pp. 2232–2242.
[36] J. Shen, *Efficient spectral-Galerkin methods* III: *Polar and cylindrical geometries*, SIAM J. Sci. Comput., 18 (1997), pp. 1583–1604.

[37] J. Shen, *Stable and efficient spectral methods in unbounded domains using Laguerre functions*, SIAM J. Numer. Anal., 38 (2000), pp. 1113–1133.
[38] G. Strang, *On the construction and comparison of difference schemes*, SIAM J. Numer. Anal., 5 (1968), pp. 506–517.
[39] G. Szegö, *Orthogonal Polynomials* 4th ed., Amer. Math. Soc. Colloq. Publ. 23, AMS, Providence, RI, 1975.
[40] T. Tang, *The Hermite spectral method for Gaussian-type functions*, SIAM J. Sci. Comput., 14 (1993), pp. 594–606.
[41] H. Yoshida, *Construction of higher order symplectic integrators*, Phys. Lett. A, 150 (1990), pp. 262–268.